Biopolymer–Lipid Bilayer Interaction Modulates the Physical Properties of Liposomes: Mechanism and Structure

ARTICLE *in* JOURNAL OF AGRICULTURAL AND FOOD CHEMISTRY · JULY 2015

Impact Factor: 2.91 · DOI: 10.1021/acs.jafc.5b01422 · Source: PubMed

7 AUTHORS, INCLUDING:

Chen Tan
Carnegie Mellon University
54 PUBLICATIONS **315** CITATIONS
SEE PROFILE

Shabbar Abbas
Jiangnan University
38 PUBLICATIONS **381** CITATIONS
SEE PROFILE

JOURNAL OF AGRICULTURAL AND FOOD CHEMISTRY

Article

pubs.acs.org/JAFC

Biopolymer−Lipid Bilayer Interaction Modulates the Physical Properties of Liposomes: Mechanism and Structure

Chen Tan, Yating Zhang, Shabbar Abbas, Biao Feng, Xiaoming Zhang, Wenshui Xia, and Shuqin Xia*

State Key Laboratory of Food Science and Technology, School of Food Science and Technology, Jiangnan University, Lihu Road 1800, Wuxi, Jiangsu 214122, China

ABSTRACT: This study was conducted to elucidate the conformational dependence of the modulating ability of chitosan, a positively charged biopolymer, on a new type of liposome composed of mixed lipids including egg yolk phosphatidylcholine (EYPC) and nonionic surfactant (Tween 80). Analysis of the dynamic and structure of bilayer membrane upon interaction with chitosan by fluorescence and electron paramagnetic resonance techniques demonstrated that, in addition to providing a physical barrier for the membrane surface, the adsorption of chitosan extended and crimped chains rigidified the lipid membrane. However, the decrease in relative microviscosity and order parameter suggested that the presence of chitosan coils disturbed the membrane organization. It was also noted that the increase of fluidity in the lipid bilayer center was not pronounced, indicating the shallow penetration of coils into the hydrophobic interior of bilayer. Microscopic observations revealed that chitosan adsorption not only affected the morphology of liposomes but also modulated the particle aggregation and fusion. Especially, a number of very heterogeneous particles were visualized, which tended to confirm the role of chitosan coils as a "polymeric surfactant". In addition to particle deformation, the membrane permeability was also tuned. These findings may provide a new perspective to understand the physiological functionality of biopolymer and design biopolymer−liposome composite structures as delivery systems for bioactive components.

KEYWORDS: *liposomes, chitosan, structure, morphology, polymeric surfactant*

INTRODUCTION

Modifying the liposomal surface via decorating with a layer or alternate deposition (layer by layer) of hydrophilic polymers has emerged as a novel way to improve liposome delivery performance. As an example, chitosan is a very promising glycosaminoglycan for biological applications due to its biocompatibility, biodegradability, and low toxicity.[1] In the field of drug delivery, nanoparticles and formulations containing chitosan have presented promising results in the search for drug release systems optimizing disease treatments and reducing drug side effects. These advantages of chitosan contribute to the development of composite phospholipid−chitosan vesicles (chitosomes) as new structures for encapsulation of drugs and vaccines aimed as vectors and tolls for controlled antigen release.[2,3] More recently, food application of chitosomes has greatly increased for encapsulating nutraceuticals to make them water-dispersible in aqueous food formulations and increase their bioavailability.[4−6]

As a soft matter, liposomes may be subjected to changes in morphology, integrity, and structure upon interaction with anchored and/or adsorbed polymers. These changes are closely related to the liposome properties, polymer characteristics, and preparation conditions. Through manipulation of these factors, chitosan can form a dense mesh covering the liposomal surface, thus improving the structural properties of liposomes, biocompatibility, and drug delivery efficiency. Interestingly, it is also argued that the strong interaction of chitosan with phospholipids may disrupt the cell membrane[7] and model liposomes,[8] thereby increasing membrane permeability.[9] The contradiction in these studies aroused our great interest to examine the mechanisms of chitosan action. One effective way is to visualize the direct response of the membrane upon interaction with chitosan. It has been revealed that the presence of chitosan negatively influences the giant unilamellar vesicles (GUVs; 1−100 μm) due to the increased spontaneous tension by chitosan adsorption,[10] whereas the effect of spontaneous tension may not necessarily occur in the case of large unilamellar vesicles (LUVs; 200−1000 nm).[11] However, what happens to the response of more highly curved vesicles (typically <200 nm) upon chitosan adsorption? More information on this issue is required in detail because such smaller vesicles have been proved to have strong adhesion and absorption into the intestinal epithelial cells for drug delivery.

Additionally, one has to consider the physical properties of polymer. It is commonly believed that at very low concentrations, the chitosan chains are fully extended and can be adsorbed flatly onto the surface of liposomal membrane, thus forming a core−shell composited structure by electrostatic interaction. However, when exceeding a certain critical aggregation concentration (CAC), chitosan could behave more like a Gaussian coil instead of the wormlike chain model by intra- and intermolecular hydrophobic interaction.[12] Therefore, chitosan and its derivatives are proposed to act as a "natural polymeric surfactant". In our recent study, we have demonstrated that as the concentration increased, the extended chains of chitosan (0−1.0 mg/mL) turned to crimp (1.0−1.5 mg/mL) and then self-aggregated, forming irregular coil (1.5−

Received: March 19, 2015
Revised: July 14, 2015
Accepted: July 14, 2015
Published: July 14, 2015

DOI: 10.1021/acs.jafc.5b01422
J. Agric. Food Chem. 2015, 63, 7277−7285

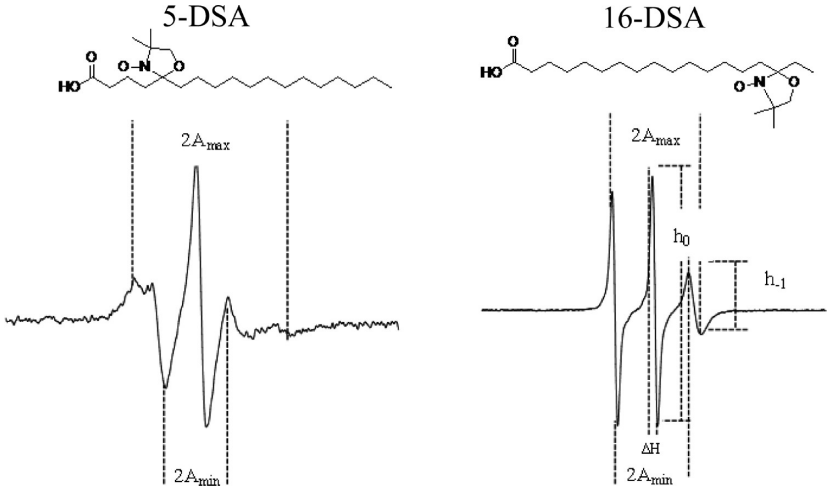

Figure 1. Molecular formula of the spin probes 5-DSA and 16-DSA and the corresponding EPR spectrum.

2.0 mg/mL) and packed coil structures (>2.0 mg/mL).[13] Such conformational change of chitosan molecules suggested that they could adopt various interaction mechanisms with liposomal membrane, besides the flat adsorption, which seemed of interest to further investigate.

On the other hand, it is important to point out that most of the suggestions aforementioned were based on a simple model membrane system composed of synthesized phospholipids. From a food industry perspective, egg yolk phosphatidylcholine (EYPC) is the commonly used lipid for the preparation of liposomes as it is a generally recognized as safe (GRAS) food ingredient. Previously, we explored a new type of liposome composed of mixed lipids including EYPC and a nonionic surfactant (Tween 80) as carriers for coenzyme Q_{10},[14,15] carotenoids,[16−19] and vitamin E.[20] The appropriate amount of Tween 80 in the formulation was demonstrated to impart high rigidity to the liposomal membrane, thus favoring the encapsulation efficiency and stability of liposomes. To the best of our knowledge, however, there is little information regarding the interaction of chitosan with mixed lipids-based liposomes.

Taken together, further detailed knowledge of such chitosan−lipid bilayer composite structure is required with special attention to the role of polymer conformation. Herein, the effect of chitosan conformation on the physical characterization of liposomes is thoroughly investigated including membrane dynamics, structure, hydrophobicity, surface morphology, and size. Several analysis techniques are introduced, including fluorescence anisotropy, electron paramagnetic resonance (EPR), transmission electron microscopy (TEM), atomic force microscopy (AFM), and dynamic light scattering (DLS). The aggregation and fusion behaviors of decorated liposomes as well as membrane permeability against surfactant are also evaluated.

MATERIALS AND METHODS

Materials. Egg yolk phospholipid (EYPC, composed of approximately 80% phosphatidylcholine, 5% lysophosphatidylcholine, and phosphatidic acid, and 15% fatty acids) was purchased from Chemical Reagent Plant of East China Normal University (Shanghai, China). Polyoxyethylene sorbitan monooleate (Tween 80) was obtained from China Medicine (Group) Shanghai Chemical Reagent Co. (Shanghai, China). Partially deacetylated chitosan (85%) with an average molecular weight of 200,000 was purchased from Ao Xing Biotechnology Co., Ltd. (Zhejiang, China). The fluorescent probe, 5(6)-carboxyfluorescein (CF), 1-[4-(trimethylammonio)phenyl]-6-phenyl-1,3,5-hexatriene (TMA-DPH, 98% purity), 8-anilino-1-naphthalenesulfonic acid (ANS, 98% purity), and the spin labels 5-doxyl-stearic acid (5-DSA) and 16-doxyl-stearic acid (16-DSA) were all purchased from Sigma Chemical Co. (St. Louis, MO, USA). All other reagents were of analytical grade.

Preparation of Chitosan-Decorated Liposomes. Bare liposomes were prepared according to our earlier method.[14] Briefly, phospholipid (6 g) and Tween 80 (4.32 g) were dissolved in 12 mL of warm ethanol at 55 °C. The ethanol solution was rapidly injected using a syringe as a pump into 120 mL of buffer solution (0.1 M acetic acid/0.01 M phosphate, 75 mM NaCl, pH 4.0) at 55 °C in a water bath under stirring at 700 rpm using an IKA RW 20 digital overhead stirrer (IKA Works Guangzhou). After agitation for 30 min, the liposomal system was transferred to a round-bottom flask attached to a rotary evaporator at 55 °C under reduced pressure to remove ethanol. The obtained liposomal suspension was then submitted to a probing sonication process in an ice bath for 10 min at 240 W with a sequence of 1 s of sonication and 1 s of rest using a sonicator (Sonics & Materials, Inc., 20 kHz). The final samples were filled into vials (the headspace of the vials was blanketed with nitrogen) and kept in a refrigerator (4 °C in the dark). The CF-entrapped liposomes were prepared in the same way expect for using 20 mM CF solution (0.1 M acetic acid/0.01 M phosphate, 75 mM NaCl, pH 4.0) instead of buffer solution. Unencapsulated CF was removed from the liposomal suspension by gel filtration through a Sephadex G-25 column.

The chitosan-decorated liposomes were prepared as follows: the chitosan was dissolved in the same buffer solution for bare liposomes and then added dropwise to bare liposomal suspension at equal volume at 1000 rpm for 30 min using an overhead stirrer at room temperature. The final concentration of chitosan was adjusted from 0.5 to 4 mg/mL. The phospholipid concentration was kept at 25 mg/mL. The final samples were filled into vials and stored at the same conditions as bare liposomes.

Liposomal Membrane Fluidity. A weighed amount of ANS probe was dissolved in ethanol solution, and the final concentration was 6×10^{-3} mol/L. The TMA-DPH stock solution was prepared by dissolving the TMA-DPH powder in tetrahydrofuran/water (1:1, v/v) and adjusting the concentration to 10^{-2} mol/L. The final TMA-DPH concentration was adjusted to 10^{-4} mol/L by PBS dilution before use. When the liposomal fluidity was determined, aliquots of probe solution were first mixed with bare liposomes in a 10 mL tube and incubated at 37 °C for 30 min. Then, different concentrations of chitosan in the same buffer were added dropwise to the incubated sample under stirring at 1000 rpm for 30 min. Note that before being mixed with liposomal samples, the ANS solution should be dried by

DOI: 10.1021/acs.jafc.5b01422
J. Agric. Food Chem. 2015, 63, 7277−7285

nitrogen to avoid the destructive effect of ethanol on liposomal membrane.

Microviscosity of liposomal membrane was measured at 25 °C using a fluorescence spectrometer (Hitachi F-7000, Japan) equipped with excitation and emission polarization filters. The excitation and emission wavelengths were, respectively, for ANS, λ_{ex} = 337 nm and λ_{em} = 480 nm and for TMA-DPH, λ_{ex} = 365 nm and λ_{em} = 430. The slit widths for both excitation and emission were 5 nm. The fluorescence intensities were measured according to our previous study.[19] The microviscosity (η) was calculated by fluorescence polarization (P) according to the equation[21]

$$\eta = 2P/(0.46 - P)$$

$$P = (I_{0,0} - GI_{0,90})/(I_{0,0} + GI_{0,90}),\ G = I_{90,0}/I_{90,90}$$

where $I_{0,0}$ and $I_{0,90}$ are the fluorescence intensities of the emitted light polarized parallel and vertical to the exciting light, respectively, and G is the grating correction coefficient.[22]

Electron Paramagnetic Resonance. The EPR technique was applied to monitor the molecular dynamics of lipids by observing the changes in the spin tropic movement of an unpaired electron. EPR measurements were performed using a Bruker EMX spectrometer (Bruker, Rheinstetten, Germany) at the X-band (9 GHz). The spectra were recorded at a microwave power of 20 mW with sweep width 120 G, center field 3511 G, and 20 s sweep time. All measurements were performed in triplicate at room temperature. In the present study, 5-DSA and 16-DSA were used as spin markers. These compounds consist of a radical group and a hydrocarbonated chain (stearic acid), which acts as a radical support (Figure 1). The radical in the 5- or 16-position of the alkyl chain will determine local motional profiles in the two main regions of the lipid bilayer, near the polar headgroup (5-DSA) or at the end of the hydrophobic chain (16-DSA). A weighed amount of 5-DSA or 16-DSA was dissolved in ethanol solution, with the final concentration adjusted to 1.0 or 0.9 mol/L, respectively. One milliliter of spin probe solution was added into a 10 mL tube followed by nitrogen dryness to remove the ethanol solution. An aliquot of 2.5 mL of bare liposomes was added into the tube and incubated at 25 °C for 30 min. Then, the chitosan solution was added dropwise to the incubated sample under stirring for 30 min.

Line widths $2A_{max}$, $2A_{min}$, and ΔH, in gauss (G), and heights of the high-field and midfield lines, h_{-1} and h_0, respectively, were obtained from the first derivative of each absorption spectrum. Spectral parameters used to study the location of spin labels in liposomal membrane are shown in Figure 1.

The order parameter (S) reflects the segmental order parameter of the segment to which the nitroxide fragment is attached.[23] It can be obtained from the conventional EPR spectra and calculated as $S = 0.5407 \times (A_{max} - A_{min})/a_0$, where $a_0 = (A_{max} + 2A_{min})/3$. The order parameter S is equal to zero for the membrane in total disorder. When it equals 1, the membrane has a crystal structure.[24]

The EPR spectrum of 16-DSA incorporated into the lipid bilayer reflects an isotropic motion of the acyl chain. In this case, rotational correlation time (τ, ns), assuming isotropic rotational diffusion of 16-DSA, can be used to measure the motion of the phospholipid acyl chains near the hydrophobic end.[25] An increase in τ indicates a decrease of membrane fluidity. It can be calculated from the following equation:

$$\tau = 6.5 \times 10^{-10} \times \Delta H \times \left(\sqrt{\frac{h_0}{h - 1}} - 1\right)$$

Transmission Electron Microscopy. TEM micrographs were performed on a Hitachi-7650 at an accelerating voltage of 200 kV. The samples (bare liposomes and chitosan-decorated liposomes) were prepared as described above. An aqueous suspension of the samples was deposited upon a carbon-coated copper grid, followed by air-drying for 1 min. Then, the sample was instantly stained with 2 wt % phosphotungstic acid for 15 s.

Atomic Force Microscopy. AFM imaging was carried out using a commercial AFM (Dimension Icon, Bruker Co., Santa Barbara, CA, USA). The ScanAsyst mode was applied using silicon tip (TESP, Bruker, nominal frequency of 320 kHz, nominal spring constant of 42 N/m) with a scan resolution of 512 samples per line. Mica sheets were freshly cleaved to obtain a flat and uniform surface and were used as the substrate for AFM observations. Just before the analysis, the liposomal samples were diluted in water to obtain a less sticky fluid. An aliquot of 1 μL of liposome suspension was deposited on the mica surface and incubated for 30 min at room temperature. Afterward, samples were carefully washed with ultrapure water to eliminate salts and nonadsorbed vesicles and dried for 24 h at room temperature. Height mode images are acquired simultaneously at a fixed scan rate (0.997 Hz) with a resolution of 512 × 512 pixels in the dimension of 5 μm × 5 μm. Processing of images and analysis was carried out using NanoScope software (Digital Instruments, version V614r1). All height images are presented after the zero-order two-dimensional flattening.

Particle Size Distribution. Size measurements were performed at 25 ± 0.1 °C using a commercial zeta-sizer (Nano-ZS90, Malvern Instruments Ltd., Worcestershire, UK) with a He/Ne laser (λ = 633 nm) and scattering angle of 90°. To evaluate the aggregation and fusion of particles, the liposomal sample was heated at 37 °C for 5 h. After heat treatment, 2 mL of liposomal dispersion was transferred into the polystyrene cuvette for size determination, and then the particle size distribution was recorded by DLS. The measurements were repeated three times.

5(6)-Carboxyfluorescein Release Study. It is generally assumed that the fluorescence emission of CF is quenched to a high extent when the molecules are encapsulated in the interior aqueous compartments of liposomes at high concentration.[26] Upon release of CF from liposomes to the bulk aqueous phase, the fluorescence intensity would increase greatly. Therefore, the release of CF was taken as a measure of the membrane permeability after the incubation of liposomes with chitosan. Briefly, an aliquot of chitosan solution (1 mL) at different concentrations was added into 1 mL of liposomal suspension. At proper time intervals, 10 μL of sample was withdrawn and diluted with 2 mL of tris buffer (50 mM, pH 7.5). The fluorescence intensity of the samples was then measured at 25 °C with a spectrofluorimeter (Hitachi F-7000, Japan) with excitation at 488 nm and emission at 520 nm. The percentage of CF release from liposomes was calculated from the equation % release = $100 \times (F_t - F_0)/(F_\infty - F_0)$, where F_0 and F_t are the fluorescence intensities of the liposome samples before and after incubation with chitosan for the time period t and F_∞ is the total flurescence intensity after liposome lysis with 10% Triton X-100. To evaluate the stability of decorated liposomes against surfactant Triton X-100, 100 μL of 10% Triton X-100 solution was added to the liposomal sample (1 mL). The CF fluorescence was immediately monitored every second by spectrofluorimeter.

Statistical Analysis. Data are presented as a mean value with its standard deviation indicated (mean ± SD). All experiments were carried out in triplicate using freshly prepared samples.

RESULTS AND DISCUSSION

Fluidity of Liposomal Membrane. The fluidity of a liposomal membrane quantitatively characterizes the mobility and molecular rotation rate of lipid.[27] Lower membrane fluidity represents a higher structural order. It is well-known that ANS and TMA-DPH serve as markers for the molecular movement on the exterior membrane surface[28] and superficial region including the surface and glycerol side-chain region,[29] respectively. The relative microviscosity η/η_0 as a function of chitosan shows that the influence of chitosan binding was more pronounced on the fluidity in membrane surface than in the glycerol side-chain region (Figure 2). As the chitosan concentration increased from 0.25 to 1.5 mg/mL, microviscosity in membrane surface region was considerably increased, but remained virtually unchanged in the superficial region. Apparently, chitosan chains mainly adsorbed to the membrane surface and restricted the motion of the polar headgroup. Notably, restriction was stronger in the case of

DOI: 10.1021/acs.jafc.5b01422
J. Agric. Food Chem. 2015, 63, 7277−7285

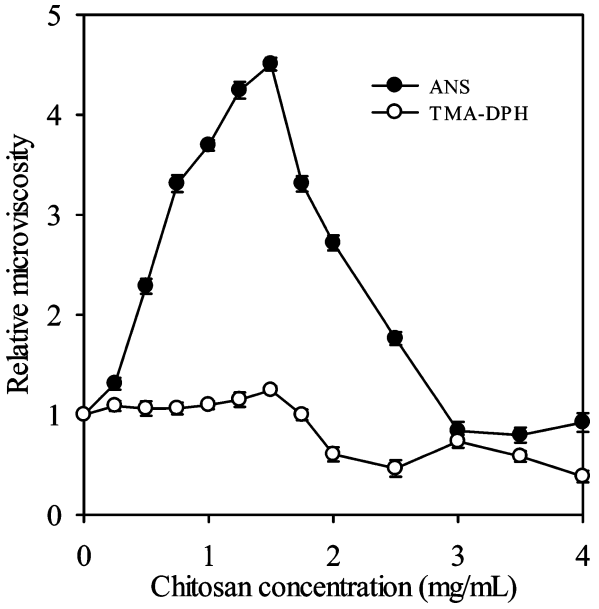

Figure 2. Relative microviscosity η/η_0 in liposomes for ANS and TMA-DPH as a function of decorated chitosan concentration. η_0 refers to the calculated microviscosity in bare liposomes, and η refers to the microviscosity in chitosan-decorated liposomes. Each point represents the mean value ± standard deviation (n = 3).

crimped chains. Considering the appearance of hydrophobic interaction accompanied by crimped chains, we speculated that besides electrostatic attraction, a weak hydrophobic force also contributed to the stabilizing effect on liposomal membrane. This hypothesis was supported by earlier research which concluded that the involvement of hydrophobic interaction could promote the physical adsorption and deposition of chitosan on membranes.[11] However, when the concentration was >1.5 mg/mL, η/η_0 values were decreased greatly surrounding ANS but only slightly surrounding TMA-DPH. This indicated that the presence of coils not only increased the fluidity of membrane surface but also somewhat disturbed the superficial region. The destabilization of chitosan coils might be correlated with the enhancement of hydrophobic interaction and, consequently, different adsorption patterns are expected instead of flat adsorption.

Motion of Alkyl Chains. EPR is a useful technique for determining the fluidity and structural changes of the lipid bilayers of liposomes. Figure 3 reveals that decoration of chitosan chains (<1.5 mg/mL) enhanced the order in the polar headgroup (at the 5-DSA position) and in the center of the bilayer (16-DSA position). This result was consistent with the Raman spectra analysis in relation to the *gauche* conformation change in the choline groups and lateral packing enhancement of the lipid chains.[19] However, the presence of chitosan coils (2.0−4.0 mg/mL) reduced the order of both regions. Combined with the high fluidizing properties, it was believed that the chitosan coils exerted a disturbing effect across the liposomal membrane. As evidenced previously, the zeta potential values were practically constant above the decorated concentration of 2 mg/mL.[13] Besides, the hydrophobic character along the chitosan chains became stronger, accompanied by the formation of chitosan coils. Therefore, it was concluded that the hydrophobic interaction prevailed in the formation of chitosan coil−liposome composites. Wydro's group[30] has also demonstrated that strong hydrophobic

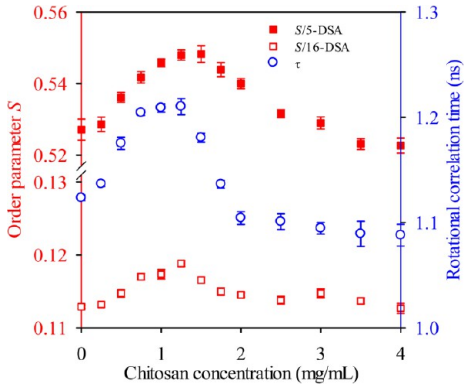

Figure 3. Order parameter S of spin probes and rotational correlation time of 16-DSA measured as a function of decorated chitosan concentration. Each point represents the mean value ± standard deviation (n = 3).

interaction between the phospholipid tails and chitosan allowed chitosan to come up to the monolayer and fill in the empty space. With these points taken into consideration, it was very likely that chitosan coils penetrated into the lipid hydrophobic core by hydrophobic interaction. On the other hand, it was noted that the disturbing effect of chitosan on the bilayer center was less pronounced than on membrane surface. This indicated that chitosan coils shallowly embedded into the one leaflet of the membrane.

Figure 3 also shows that the correlation time of 16-DSA free radical moiety increased from 0.25 to 1.5 mg/mL, whereas beyond this range, it was considerably decreased. This indicated that the segmental motion of the alkyl chains was restricted by the binding of chitosan chains, whereas chitosan coils failed to restrict the motion of the alkyl chains. The fluidizing property of chitosan deduced from correlation time was well in accordance with the results of membrane fluidity. On the basis of the analysis of membrane fluidity and structure, it was believed that besides providing a physical barrier, chitosan chains also exerted a rigidifying effect on the lipid membrane. Through modifying the membrane fluidity and ordering state, chitosan could mediate the permeation of foreign molecules into the membrane, thereby exhibiting a stabilizing role in liposome. These advantages of chitosan contribute to the development of composite phospholipid−chitosan vesicles (chitosomes) as new structures for the encapsulation of drugs and nutraceuticals.

Membrane Hydrophobicity. The isotropic hyperfine coupling constant a_0 of 5-DSA and 16-DSA was measured to determine the hydrophobicity of the polar headgroup region of the membrane and hydrophobic core, respectively. A decrease of the a value indicates an increase of hydrophobicity at the spin label position.[31] The hydrophobicity of the membrane headgroup region did not vary when the chitosan concentration was <0.5 mg/mL, whereas it was greatly increased in the range of 0.75−1.5 mg/mL (Figure 4). Apparently, the coated layer of chitosan chains can effectively increase the activation energy for polar small molecules to get across the membrane. Furthermore, the thicker the coated layer formed by the crimped chains, the higher was the physical barrier against the penetration of polar molecules. Another reason for the high hydrophobicity was that the decoration of crimped chains rigidified the organization of phospholipids at the polar headgroup and decreased the membrane permeability. These

DOI: 10.1021/acs.jafc.5b01422
J. Agric. Food Chem. 2015, 63, 7277−7285

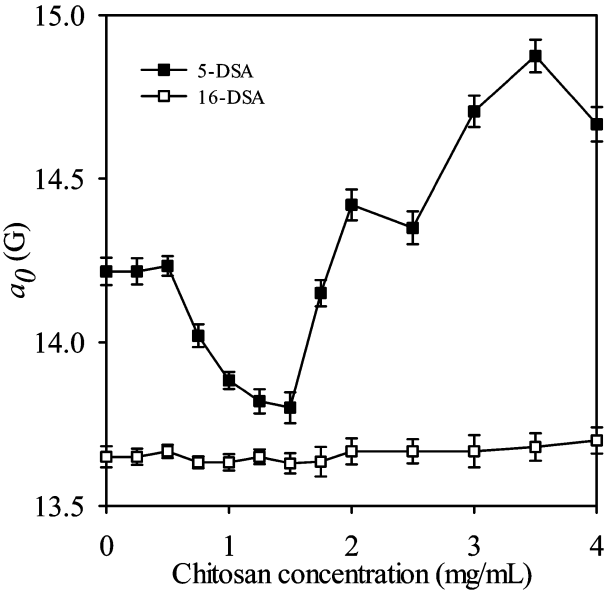

Figure 4. Isotropic hyperfine coupling constant a_0 of 5-DSA and 16-DSA in chitosan-decorated liposomes as a function of concentration. Each point represents the mean value ± standard deviation (n = 3).

mechanisms may contribute to the controlled release of encapsulated compounds in vehicles by decreasing water penetration.[32,33] However, a sudden increase in the a_0 values of 5-DSA was observed as the concentration was increased to 1.5 mg/mL. This phenomenon was understandable because the chitosan coils tended to penetrate into the liposomal membrane, rather than flat adsorption. Consequently, the polar region of the membrane was loosened, and more additional space was available for water penetration. By contrast, the effect of chitosan decoration on the hydrophobicity of membrane bilayer core was not pronounced, with a slight increase in a_0 values of 16-DSA from 1.75 mg/mL. In combination with the small influence of chitosan decoration on the fluidity of bilayer centre, this observation further confirmed the shallow insertion of chitosan coils, thus practically preserving the hydrophobic barrier of bilayer core.

Liposome Morphology. Alteration of adsorption behavior is always accompanied by a change in mechanisms of membrane deformation.[34] The morphological characterization of bare liposomes and chitosan-decorated liposomes was visualized by TEM after negative staining (Figure 5). It can be seen that bare particles were spherical. After decoration by chitosan, a different trend in morphological change was observed. At chitosan concentrations of 1.0, 1.5, and 2.0 mg/mL, the composite particles seemed to exhibit rectangular shape but maintained relatively monodispersion. The particle size was roughly in the range of 70−150 nm. The size observed from the microscopic images was somewhat greater than that determined using DLS technique.[13] This difference may have been related to the artifact effect of the analytical methods. For instance, the light-scattering instrument requires the high dilution of samples prior to analysis, which may have changed the particle size of the samples.[35] On the other hand, a very thin

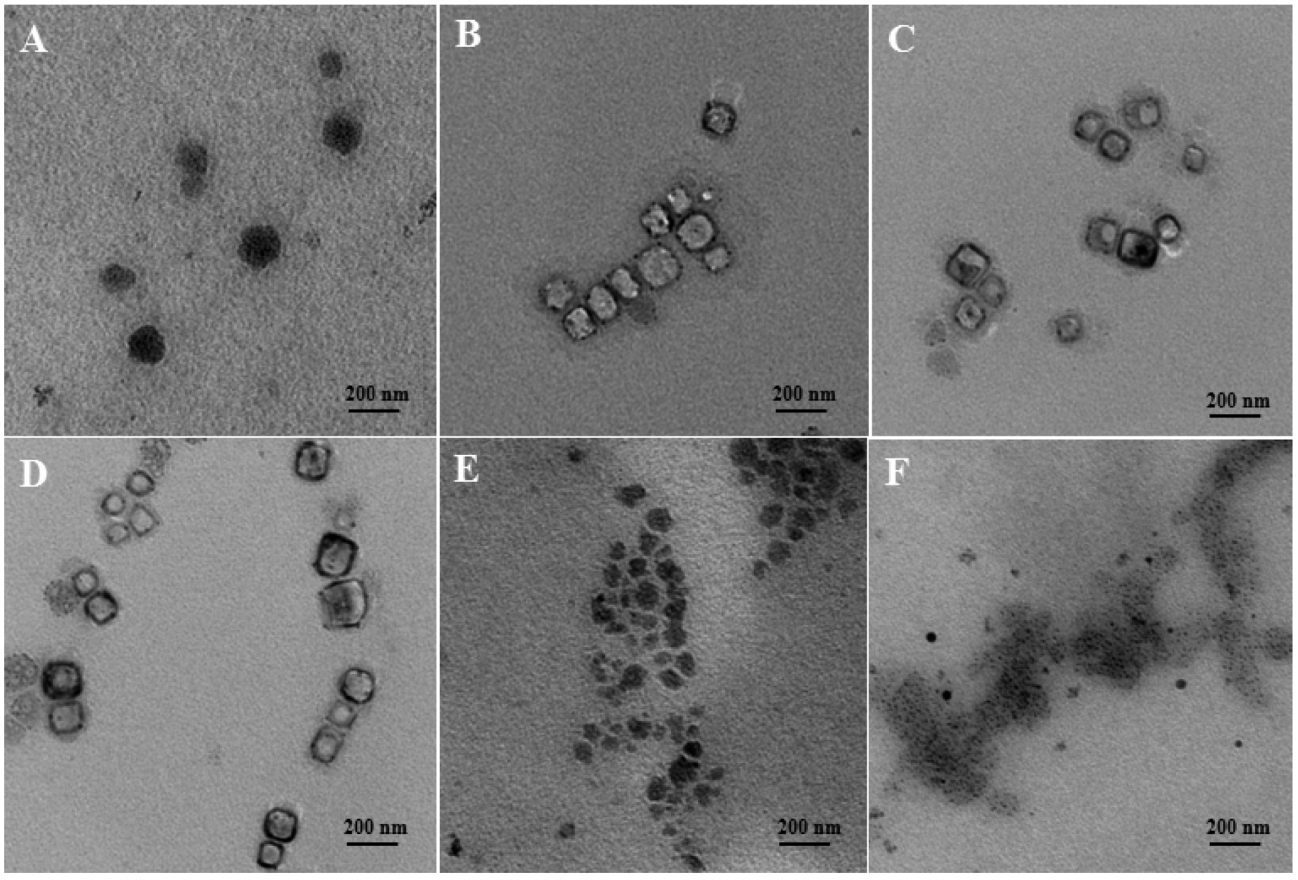

Figure 5. Transmission electron micrographs of bare liposomes (A) and liposomes decorated by chitosan at 1.0 mg/mL (B), 1.5 mg/mL (C), 2.0 mg/mL (D), 3.0 mg/mL (E), and 4.0 mg/mL (F).

DOI: 10.1021/acs.jafc.5b01422
J. Agric. Food Chem. 2015, 63, 7277−7285

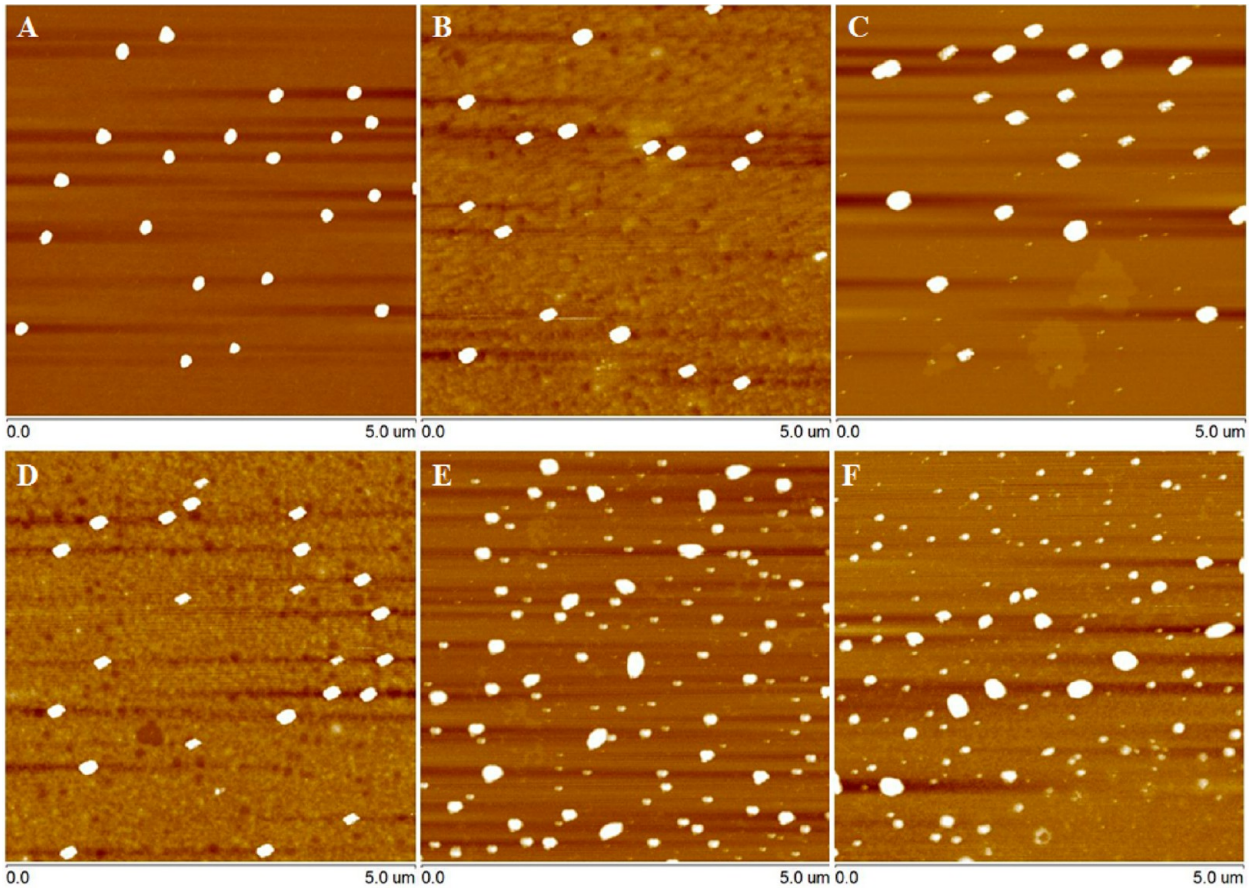

Figure 6. Scan Asyst mode AFM images of bare liposomes and liposomes decorated by chitosan at concentrations of 1.0, 1.5, 2.0, 3.0, and 4.0 mg/mL. The study was performed immediately after the preparation. Scan size = 5 μm × 5 μm.

coated layer (~10 nm) around the liposomal particles can be observed, demonstrating the interaction of chitosan with liposomes as well as the flat adsorption of chitosan chains.[13] The dimension and charged property of the system also revealed an electrostatic interaction that, after titration with chitosan to attain a concentration of 0.5 mg/mL, increased the average diameter of liposomes from 82.9 to 90 nm, with a charge inversion from −17.9 (bare liposomes) to 10.6 (decorated liposomes).[13] However, with further increase of chitosan concentration (from 3.0 to 4.0 mg/mL), the suspension became very heterogeneous and the shape of the particles was completely distorted (Figure 5E,F). Many small particles (<50 nm) were found in the field of vision. Diameter distribution analysis provided a complementary picture of a strong volume peak of liposomes located in the range of 10−50 nm in the presence of chitosan coils.[13]

AFM images of bare liposomes and chitosan-decorated liposomes are shown in Figure 6. The majority of bare liposomes maintained a spherical and well-defined shape. The presence of chitosan led to a change in the shape of liposomes, depending upon the chitosan concentration. The shape of liposomes appeared rectangular at concentrations of 1.0, 1.5, and 2.0 mg/mL, but was more irregular at 3.0 and 4.0 mg/mL. This observation supported the results obtained by TEM analysis. Deformation of particles observed from AFM images could be attributed to different factors, such as particle collapse during evaporation[36] and interactions of adsorbed polymer with supported surface.[10] In our case, it appeared that the original morphology of liposome was not significantly influenced by the spontaneous collapse, as evidenced from the fairly spherical shape of bare liposomes (Figure 6A).

In combination with TEM observation, the morphological alteration of liposomes has to be related to the modification of chitosan on the lipid headgroup. Upon binding of chitosan to the surface of small vesicles, the chitosan chain would bend to adapt to the large curvature of the sphere. This process probably, in turn, builds tension in the membrane and increases the spontaneous curvature of the bilayer. This phenomenon brought about the change in morphology. Moreover, if the binding of polyelectrolyte becomes stronger, the membrane would be subjected to a higher degree of bending.[34] Thus, the deformation of liposomes was more apparent in the presence of crimped chains (at 1.5 and 2.0 mg/mL). It was also possible that the hydrophobic residues of crimped chains incorporated into the membrane interior and occupied the position of phospholipid molecules. As a result, a portion of lipid acyl chains orientated toward higher curvature, leading particles to be elongated.[37] At higher chitosan concentrations (3.0 and 4.0 mg/mL), a number of very heterogeneous particles were visible, which may be generated probably due to the reorganization of particles subsequent to collapse. This observation can be explained by the fact that chitosan coils progressively penetrated into the lipid bilayer until disrupting it. At this stage, the hydrophobic interaction was intensified, accompanying the formation of chitosan coils. The almost unchanged zeta potential values of the system (>2 mg/mL) also confirmed the existence of hydrophobic interaction.[13] Therefore, it was believed that the main forces involved were

DOI: 10.1021/acs.jafc.5b01422
J. Agric. Food Chem. 2015, 63, 7277−7285

hydrophobic in nature, as demonstrated by the incorporation of surfactant molecules into the phospholipid bilayer.[38] If the main aim of chitosan modification was to stabilize liposome, high concentrations at which chitosan adopted coil conformation should be avoided, considering the lipid bilayer membrane disruption. On the other hand, the "polymeric surfactant" property of chitosan provided us a new perspective to elucidate that the ability of chitosan to disrupt the lipid bilayer membrane for the antimicrobial[39] and biological activity[40] partially related to its coil conformation.

Aggregation and Fusion of Liposomes. The susceptibility of liposome to aggregation or fusion during production, storage, transport, and after administration is highly challenging.[41] Here, we briefly discuss the observations on the aggregation and fusion of the composite chitosan−lipid particles after heat treatment.

Analysis on the particle size using DLS technique showed that there was only a single volume peak observed for the chitosan-decorated liposomes at 1.0, 1.5, and 2.0 mg/mL after 5 h of incubation at 37 °C (Figure 7). This indicated that the

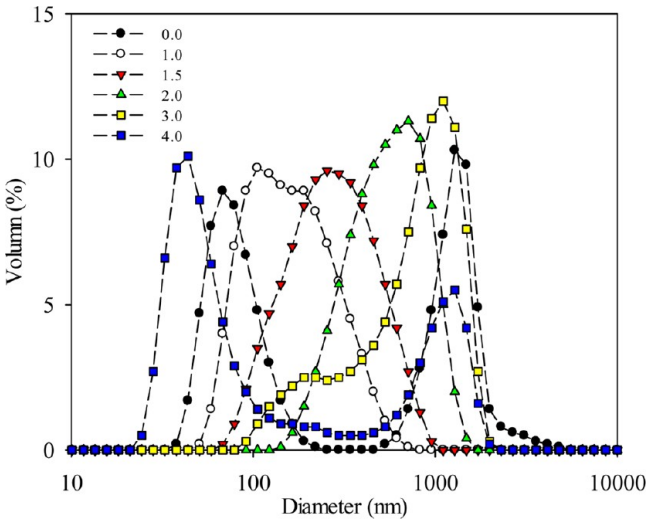

Figure 7. Diameter distribution of bare liposomes and chitosan-decorated liposome after 5 h of incubation at 37 °C.

suspensions can maintain the homogeneous distribution even though they were heated. However, bimodal distribution occurred for uncoated liposomes and liposomes decorated by chitosan of 3.0 and 4.0 mg/mL. It is very likely that the volume peak located at large diameter (around 1100 nm) was caused by the particle aggregation or fusion.

AFM measurement provided direct visualization of the aggregated and fused behavior of particles (Figure 8). In the absence of chitosan, particles adhered to each other after incubation. The diameter of fused particles ranged from 295 to 957 nm. After decoration by chitosan at 1.0 and 1.5 mg/mL, few particles aggregated together and the boundary of the unit particle was clearly observed. It was believed that the combining effect of electrostatic repulsion and steric hindrance by externally adsorbed polymers inhibited particle aggregation. However, decoration of high chitosan concentration induced the aggregation and fusion. We can observe that four or five individual particles adhered to each other, forming bigger aggregates in the whole vision field (Figure 8D). This interesting phenomenon might be associated with the bridging effect of chitosan-bound chains to neighboring vesicles.[11] The aggregated liposomes fused into a single liposome resembling the shape of a distorted rod or an elongated sphere (Figure 8E) or into large irregular clusters (Figure 8F). The lateral segregation of the anionic lipid by polyelectrolyte adsorption and consequently disordered lipid packing could be a possible reason for liposome fusion.[42] In addition, a low level of membrane fluidity was supposed to prevent particle aggregation effectively, whereas it behaved oppositely at high fluidity.[43] Thus, liposome aggregation was also readily understandable when correlated with the analysis on fluorescence anisotropy (Figure 2).

Liposomal Membrane Permeability. To understand whether the interaction of chitosan affected membrane permeability, leakage of CF from liposomes was monitored during the interaction process of chitosan and liposomes. Figure 9A shows that bare liposomes (0.0 mg/mL) spontaneously released very small amounts of encapsulated CF due to instability. After liposomes had been incubated with chitosan in the range of 0.5−1.5 mg/mL, the release profile of CF was not significantly affected. Only when incubation time exceeded 15 min were the leaked amounts of CF from decorated liposomes lower than that from bare liposomes, suggesting the gradual formation of a chitosan layer. This process also implied that although the morphology was modified by chitosan, the permeability of the membrane was not significantly altered. However, once the chitosan concentration increased (2.0−4.0 mg/mL), a progressive and higher leakage of CF appeared. This observation demonstrated that the interaction process of chitosan coils with liposomes was accompanied by the penetration of chitosan coils into the membrane.

The physicochemical barrier of the lipid bilayer against the penetration of foreign elements plays a key role in protecting the incorporated bioactive components. To evaluate the rigidity of liposomal particles, their resistance against surfactant Triton X-100 was carried out. Figure 9B shows that the release of CF from bare liposomes increased dramatically, as around 30% of encapsulated CF molecules leaked after 120 s. It was suggested that a large amount of Triton X-100 penetrated into the bilayer and initiated the solubilization process. Liposomes decorated by chitosan ranging from 0.5 to 1.5 mg/mL possessed higher durability against Triton X-100 penetration and maintained the release rate at a low level. The strong resistance could be due to the dense mesh covering the membrane surface and rigidification of chitosan. Conversely, liposome membrane decorated by a high concentration of chitosan became more permeable to surfactant, as observed from serious leakage of CF. After 120 s of incubation, around 30, 35, and 38% of CF leaked from liposomes decorated by 2.0, 3.0, and 4.0 mg/mL chitosan, respectively, confirming the destabilizing effect of chitosan coils.

Conclusion. In the present study, we have demonstrated the contrasting modulations of chitosan on the dynamics, structure, hydrophobicity, morphology, and permeability of liposomal membrane. The extended and crimped chains of chitosan not only provided a physical barrier to the liposome surface but also rigidified the lipid membrane. Although the morphology was altered by chitosan decoration, the membrane permeability was preserved or decreased. Such characteristics make these composite vesicles potential candidates for an efficient delivery system for drugs and nutraceuticals. However, chitosan coils displayed a "polymer surfactant" nature by penetrating into the interior of lipid bilayer. These destabilizing

DOI: 10.1021/acs.jafc.5b01422
J. Agric. Food Chem. 2015, 63, 7277−7285

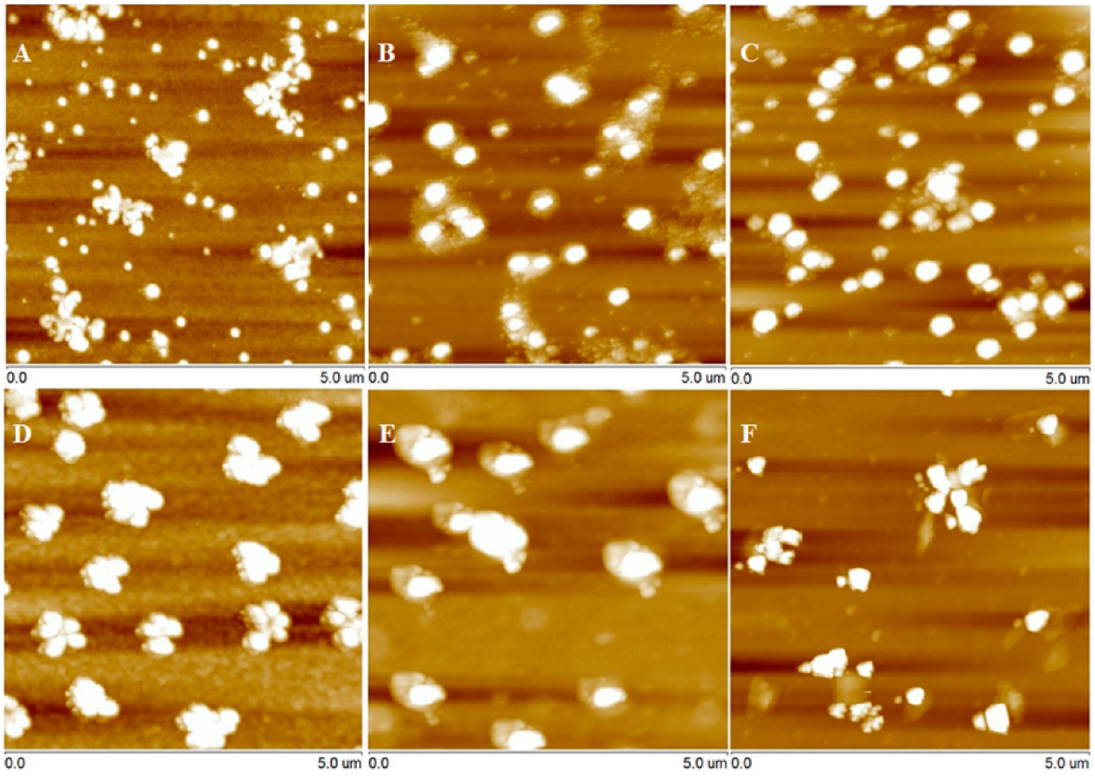

Figure 8. Scan Asyst mode AFM images of bare liposomes (A) and liposomes decorated by chitosan at concentrations of 1.0 mg/mL (B), 1.5 mg/mL (C), 2.0 mg/mL (D), 3.0 mg/mL (E), and 4.0 mg/mL (F). The study was performed after 5 h of incubation at 37 °C. Scan size = 5 μm × 5 μm.

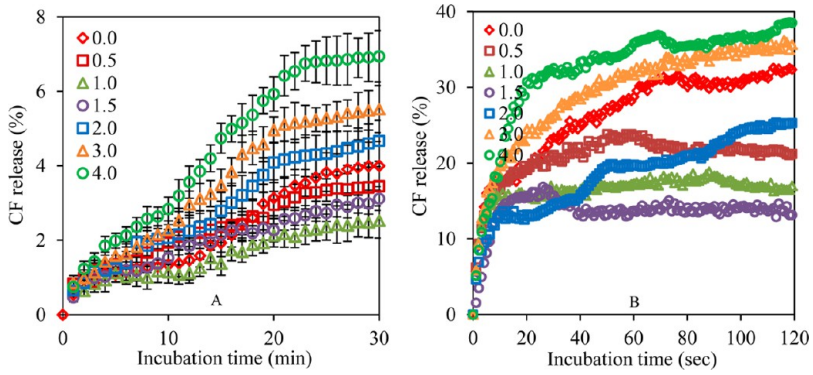

Figure 9. Time course of CF release kinetic from bare liposomes after exposure to chitosan of different concentrations (A) or from chitosan-decorated liposomes after exposure to Triton X-100 (B). When Triton X-100 was added to the suspension, the CF fluorescence was immediately monitored every second by a spectrofluorimeter.

effects of coils implied the ability of chitosan to disrupt cell membranes and the infeasibility in the design of nutraceutical delivery systems.

AUTHOR INFORMATION

Corresponding Author

*(S.X.) E-mail: sqxia2006@hotmail.com. Phone: +86-510-85884496. Fax: +86-510-85884496.

Funding

This research was financially supported by projects of the National Science Foundation of China (31471624) and the Natural Science Foundation of Jiangsu Province (BK 20141111) and by 111 Project B07029.

Notes

The authors declare no competing financial interest.

REFERENCES

(1) Elsabee, M. Z.; Morsi, R. E.; Al-Sabagh, A. M. Surface active properties of chitosan and its derivatives. *Colloids Surf., B* **2009**, *74*, 1−16.

(2) Gonçalves, M. C.; Mertins, O.; Pohlmann, A. R.; Silveira, N. P.; Guterres, S. S. Chitosan coated liposomes as an innovative nanocarrier for drugs. *J. Biomed. Nanotechnol.* **2012**, *8*, 240−250.

(3) Lee, J.-H.; Oh, H.; Baxa, U.; Raghavan, S. R.; Blumenthal, R. Biopolymer-connected liposome networks as injectable biomaterials capable of sustained local drug delivery. *Biomacromolecules* **2012**, *13*, 3388−3394.

(4) Shin, G. H.; Chung, S. K.; Kim, J. T.; Joung, H. J.; Park, H. J. Preparation of chitosan-coated nanoliposomes for improving the mucoadhesive property of curcumin using the ethanol injection method. *J. Agric. Food Chem.* **2013**, *61*, 11119−11126.

(5) Madrigal-Carballo, S.; Lim, S.; Rodriguez, G.; Vila, A. O.; Krueger, C. G.; Gunasekaran, S.; Reed, J. D. Biopolymer coating of

DOI: 10.1021/acs.jafc.5b01422
J. Agric. Food Chem. 2015, 63, 7277−7285

soybean lecithin liposomes via layer-by-layer self-assembly as novel delivery system for ellagic acid. *J. Funct. Foods* **2010**, *2*, 99−106.
(6) Panya, A.; Laguerre, M.; Lecomte, J.; Villeneuve, P.; Weiss, J.; McClements, D. J.; Decker, E. A. Effects of chitosan and rosmarinate esters on the physical and oxidative stability of liposomes. *J. Agric. Food Chem.* **2010**, *58*, 5679−5684.
(7) Helander, I.; Nurmiaho-Lassila, E.-L.; Ahvenainen, R.; Rhoades, J.; Roller, S. Chitosan disrupts the barrier properties of the outer membrane of Gram-negative bacteria. *Int. J. Food Microbiol.* **2001**, *71*, 235−244.
(8) Fang, N.; Chan, V.; Mao, H.-Q.; Leong, K. W. Interactions of phospholipid bilayer with chitosan: effect of molecular weight and pH. *Biomacromolecules* **2001**, *2*, 1161−1168.
(9) Young, D. H.; Köhle, H.; Kauss, H. Effect of chitosan on membrane permeability of suspension-cultured *Glycine max* and *Phaseolus vulgaris* cells. *Plant Physiol.* **1982**, *70*, 1449−1454.
(10) Mertins, O.; Dimova, R. Insights on the interactions of chitosan with phospholipid vesicles. Part II: Membrane stiffening and pore formation. *Langmuir* **2013**, *29*, 14552−14559.
(11) Mertins, O.; Dimova, R. Binding of chitosan to phospholipid vesicles studied with isothermal titration calorimetry. *Langmuir* **2011**, *27*, 5506−5515.
(12) Pepić, I.; Filipović-Grčić, J.; Jalšenjak, I. Interactions in a nonionic surfactant and chitosan mixtures. *Colloids Surf., A* **2008**, *327*, 95−102.
(13) Tan, C.; Xue, J.; Eric, K.; Feng, B.; Zhang, X.; Xia, S. Dual effects of chitosan decoration on the liposomal membrane physicochemical properties as affected by chitosan concentration and molecular conformation. *J. Agric. Food Chem.* **2013**, *61*, 6901−6910.
(14) Xia, S.; Xu, S.; Zhang, X.; Zhong, F. Effect of coenzyme Q10 incorporation on the characteristics of nanoliposomes. *J. Phys. Chem. B* **2007**, *111*, 2200−2207.
(15) Xia, S.; Xu, S.; Zhang, X. Optimization in the preparation of coenzyme Q10 nanoliposomes. *J. Agric. Food Chem.* **2006**, *54*, 6358−6366.
(16) Tan, C.; Zhang, Y.; Abbas, S.; Feng, B.; Zhang, X.; Xia, S. Modulation of the carotenoid bioaccessibility through liposomal encapsulation. *Colloids Surf., B* **2014**, *123*, 692−700.
(17) Tan, C.; Xue, J.; Abbas, S.; Feng, B.; Zhang, X.; Xia, S. Liposome as a delivery system for carotenoids: comparative antioxidant activity of carotenoids as measured by ferric reducing antioxidant power, DPPH assay and lipid peroxidation. *J. Agric. Food Chem.* **2014**, *62*, 6726−6735.
(18) Tan, C.; Xue, J.; Lou, X.; Abbas, S.; Guan, Y.; Feng, B.; Zhang, X.; Xia, S. Liposomes as delivery systems for carotenoids: comparative studies of loading ability, storage stability and in vitro release. *Food Funct.* **2014**, *5*, 1232−1240.
(19) Tan, C.; Xia, S.; Xue, J.; Xie, J.; Feng, B.; Zhang, X. Liposomes as vehicles for lutein: preparation, stability, liposomal membrane dynamics, and structure. *J. Agric. Food Chem.* **2013**, *61*, 8175−8184.
(20) Xia, S.; Tan, C.; Xue, J.; Lou, X.; Zhang, X.; Feng, B. Chitosan/tripolyphosphate-nanoliposomes core-shell nanocomplexes as vitamin E carriers: shelf-life and thermal properties. *Int. J. Food Sci. Technol.* **2014**, *49*, 1367−1374.
(21) Shinitzky, M.; Barenholz, Y. Fluidity parameters of lipid regions determined by fluorescence polarization. *Biochim. Biophys. Acta, Rev. Biomembr.* **1978**, *515*, 367−394.
(22) Imura, T.; Sakai, H.; Yamauchi, H.; Kaise, C.; Kozawa, K.; Yokoyama, S.; Abe, M. Preparation of liposomes containing Ceramide 3 and their membrane characteristics. *Colloids Surf., B* **2001**, *20*, 1−8.
(23) Subczynski, W. K.; Markowska, E.; Gruszecki, W. I.; Sielewiesiuk, J. Effects of polar carotenoids on dimyristoylphosphatidylcholine membranes: a spin-label study. *Biochim. Biophys. Acta, Biomembr.* **1992**, *1105*, 97−108.
(24) Gordon, L. M.; Sauerheber, R. D.; Esgate, J. A. Spin label studies on rat liver and heart plasma membranes: Effects of temperature, calcium, and lanthanum on membrane fluidity. *J. Supramol. Struct.* **1978**, *9*, 299−326.
(25) Coderch, L.; Fonollosa, J.; De Pera, M.; Estelrich, J.; De La Maza, A.; Parra, J. L. Influence of cholesterol on liposome fluidity by EPR: Relationship with percutaneous absorption. *J. Controlled Release* **2000**, *68*, 85−95.
(26) De la Maza, A.; Parra, J.; Sanchez Leal, J. Alteration of permeability of neutral and electronegatively charged liposomes by alkyl sulfate surfactants. *Langmuir* **1992**, *8*, 2422−2426.
(27) Lee, H.; Kim, H. R.; Park, J. C. Dynamics and stability of lipid bilayers modulated by thermosensitive polypeptides, cholesterols, and PEGylated lipids. *Phys. Chem. Chem. Phys.* **2014**, *16*, 3763−3770.
(28) Marczak, A. Fluorescence anisotropy of membrane fluidity probes in human erythrocytes incubated with anthracyclines and glutaraldehyde. *Bioelectrochemistry* **2009**, *74*, 236−239.
(29) Prendergast, F. G.; Haugland, R. P.; Callahan, P. J. 1-[4-(Trimethylamino)phenyl]-6-phenylhexa-1,3,5-triene: synthesis, fluorescence properties and use as a fluorescence probe of lipid bilayers. *Biochemistry* **1981**, *20*, 7333−7338.
(30) Wydro, P.; Krajewska, B.; Hąc-Wydro, K. Chitosan as a lipid binder: a langmuir monolayer study of chitosan−lipid interactions. *Biomacromolecules* **2007**, *8*, 2611−2617.
(31) Wisniewska, A.; Widomska, J.; Subczynski, W. K. Carotenoid-membrane interactions in liposomes: effect of dipolar, monopolar, and nonpolar carotenoids. *Acta Biochim. Polym.* **2006**, *53*, 475−484.
(32) Lis, M.; Wizert, A.; Przybylo, M.; Langner, M.; Swiatek, J.; Jungwirth, P.; Cwiklik, L. The effect of lipid oxidation on the water permeability of phospholipids bilayers. *Phys. Chem. Chem. Phys.* **2011**, *13*, 17555−17563.
(33) Lee, Y.-H.; Mei, F.; Bai, M.-Y.; Zhao, S.; Chen, D.-R. Release profile characteristics of biodegradable-polymer-coated drug particles fabricated by dual-capillary electrospray. *J. Controlled Release* **2010**, *145*, 58−65.
(34) McMahon, H. T.; Gallop, J. L. Membrane curvature and mechanisms of dynamic cell membrane remodelling. *Nature* **2005**, *438*, 590−596.
(35) Salvia-Trujillo, L.; Qian, C.; Martín-Belloso, O.; McClements, D. J. Influence of particle size on lipid digestion and β-carotene bioaccessibility in emulsions and nanoemulsions. *Food Chem.* **2013**, *141*, 1472−1480.
(36) Pentak, D. Physicochemical properties of liposomes as potential anticancer drugs carriers. Interaction of etoposide and cytarabine with the membrane: spectroscopic studies. *Spectrochim. Acta, Part A* **2014**, *122*, 451−460.
(37) Peter, B. J.; Kent, H. M.; Mills, I. G.; Vallis, Y.; Butler, P. J. G.; Evans, P. R.; McMahon, H. T. BAR domains as sensors of membrane curvature: the amphiphysin BAR structure. *Science* **2004**, *303*, 495−499.
(38) De la Maza, A.; Parra, J. L.; Sanchez Leal, J. Alteration of permeability of neutral and electronegatively charged liposomes by alkyl sulfate surfactants. *Langmuir* **1992**, *8*, 2422−2426.
(39) Kong, M.; Chen, X. G.; Xing, K.; Park, H. J. Antimicrobial properties of chitosan and mode of action: a state of the art review. *Int. J. Food Microbiol.* **2010**, *144*, 51−63.
(40) Pavinatto, F. J.; Pavinatto, A.; Caseli, L.; dos Santos, D. S.; Nobre, T. M.; Zaniquelli, M. E. D.; Oliveira, O. N. Interaction of chitosan with cell membrane models at the air−water interface. *Biomacromolecules* **2007**, *8*, 1633−1640.
(41) Takeuchi, H.; Kojima, H.; Yamamoto, H.; Kawashima, Y. Evaluation of circulation profiles of liposomes coated with hydrophilic polymers having different molecular weights in rats. *J. Controlled Release* **2001**, *75*, 83−91.
(42) Brender, J. R.; Hartman, K.; Gottler, L. M.; Cavitt, M. E.; Youngstrom, D. W.; Ramamoorthy, A. Helical conformation of the SEVI precursor peptide $PAP_{248-286}$, a dramatic enhancer of HIV infectivity, promotes lipid aggregation and fusion. *Biophys. J.* **2009**, *97*, 2474−2483.
(43) Heurtault, B.; Saulnier, P.; Pech, B.; Proust, J.-E.; Benoit, J.-P. Physico-chemical stability of colloidal lipid particles. *Biomaterials* **2003**, *24*, 4283−4300.

DOI: 10.1021/acs.jafc.5b01422
J. Agric. Food Chem. 2015, 63, 7277−7285